

Electrochemical derusting in molten $\text{Na}_2\text{CO}_3\text{-K}_2\text{CO}_3$

Dong-yang Zhang, Xue Ma, Hong-wei Xie, Xiang Chen, Jia-kang Qu, Qiu-shi Song, and Hua-yi Yin

Cite this article as:

Dong-yang Zhang, Xue Ma, Hong-wei Xie, Xiang Chen, Jia-kang Qu, Qiu-shi Song, and Hua-yi Yin, Electrochemical derusting in molten $\text{Na}_2\text{CO}_3\text{-K}_2\text{CO}_3$, *Int. J. Miner. Metall. Mater.*, 28(2021), No. 4, pp. 637-643. <https://doi.org/10.1007/s12613-020-2068-2>

View the article online at [SpringerLink](#) or [IJMMM Webpage](#).

Articles you may be interested in

Dong Wang, Sheng Pang, Chun-yue Zhou, Yan Peng, Zhi Wang, and Xu-zhong Gong, [Improve titanate reduction by electro-deoxidation of \$\text{Ca}_3\text{Ti}_2\text{O}_7\$ precursor in molten \$\text{CaCl}_2\$](#) , *Int. J. Miner. Metall. Mater.*, 27(2020), No. 12, pp. 1618-1625. <https://doi.org/10.1007/s12613-020-2165-2>

Chun-fa Liao, Yun-fen Jiao, Xu Wang, Bo-qing Cai, Qiang-chao Sun, and Hao Tang, [Electrical conductivity optimization of the \$\text{Na}_3\text{AlF}_6\text{-Al}_2\text{O}_3\text{-Sm}_2\text{O}_3\$ molten salts system for Al-Sm intermediate binary alloy production](#), *Int. J. Miner. Metall. Mater.*, 24(2017), No. 9, pp. 1034-1042. <https://doi.org/10.1007/s12613-017-1493-3>

Bo Wang, Chao-yi Chen, Jun-qi Li, Lin-zhu Wang, Yuan-pei Lan, and Shi-yu Wang, [Solid oxide membrane-assisted electrolytic reduction of \$\text{Cr}_2\text{O}_3\$ in molten \$\text{CaCl}_2\$](#) , *Int. J. Miner. Metall. Mater.*, 27(2020), No. 12, pp. 1626-1634. <https://doi.org/10.1007/s12613-020-2141-x>

Shu-mei Chen, Chun-fa Liao, Jue-yuan Lin, Bo-qing Cai, Xu Wang, and Yun-fen Jiao, [Electrical conductivity of molten \$\text{LiF-DyF}_3\text{-Dy}_2\text{O}_3\text{-Cu}_2\text{O}\$ system for Dy-Cu intermediate alloy production](#), *Int. J. Miner. Metall. Mater.*, 26(2019), No. 6, pp. 701-709. <https://doi.org/10.1007/s12613-019-1775-z>

Wei Liu, Qing-he Zhao, and Shuan-zhu Li, [Relationship between the specific surface area of rust and the electrochemical behavior of rusted steel in a wet-dry acid corrosion environment](#), *Int. J. Miner. Metall. Mater.*, 24(2017), No. 1, pp. 55-63. <https://doi.org/10.1007/s12613-017-1378-5>

Dong-liang Li, Gui-qin Fu, Miao-yong Zhu, Qing Li, and Cheng-xiang Yin, [Effect of Ni on the corrosion resistance of bridge steel in a simulated hot and humid coastal-industrial atmosphere](#), *Int. J. Miner. Metall. Mater.*, 25(2018), No. 3, pp. 325-338. <https://doi.org/10.1007/s12613-018-1576-9>



IJMMM WeChat



QQ author group

Electrochemical derusting in molten $\text{Na}_2\text{CO}_3\text{--K}_2\text{CO}_3$

Dong-yang Zhang¹), Xue Ma¹), Hong-wei Xie¹), Xiang Chen¹), Jia-kang Qu¹), Qiu-shi Song¹),
and Hua-yi Yin^{1,2})

1) Key Laboratory for Ecological Metallurgy of Multimetallic Mineral of Ministry of Education, School of Metallurgy, Northeastern University, Shenyang 110819, China

2) Key Laboratory of Data Analytics and Optimization for Smart Industry of Ministry of Education, Northeastern University, Shenyang 110819, China

(Received: 27 December 2019; revised: 12 April 2020; accepted: 13 April 2020)

Abstract: The formation of a rust layer on iron and steels surfaces accelerates their degradation and eventually causes material failure. In addition to fabricating a protective layer or using a sacrificial anode, repairing or removing the rust layer is another way to reduce the corrosion rate and extend the lifespans of iron and steels. Herein, an electrochemical healing approach was employed to repair the rust layer in molten $\text{Na}_2\text{CO}_3\text{--K}_2\text{CO}_3$. The rusty layers on iron rods and screws were electrochemically converted to iron in only several minutes and a metallic luster appeared. Scanning electron microscopy (SEM) and energy dispersive X-ray spectroscopy (EDS) analyses showed that the structures of the rust layer after healing were slightly porous and the oxygen content reached a very low level. Thus, high-temperature molten-salt electrolysis may be an effective way to metalize iron rust of various shapes and structures in a short time, and could be used in the repair of cultural relics and even preparing a three-dimensional porous structures for other applications.

Keywords: molten salt; electro-deoxidation; rust; stainless steel; derusting

1. Introduction

Iron and steels are the most widely used metals in modern society [1]. Ideally, to achieve corrosion resistance, a dense oxide scale is applied to the surface of metals. However, a rust layer often appears on the surfaces of iron and steels when they react with oxygen in natural or extremely corrosive environments, which causes the degradation of these metals [2]. Conventional methods for dealing with corrosion are to fabricate a protective layer, establish a connection with a sacrificial anode, or modify the surface [3]. Although these approaches can slow the rate of corrosion, corrosion is still inevitable. Apart from corrosion protection, corrosion remediation may offer an alternative approach to mitigating corrosion by rehabilitating iron and steels. Derusting methods can be divided into two categories: chemical and physical [4–7]. Chemical derusting methods remove rust by dissolving iron rust in acid solutions. This approach is facile and low in cost, but generates secondary wastes and causes hydrogen embrittlement of the iron and steels. Physical methods remove rust by external physical forces such as polishing, flame cleaning, grit blasting, sand blasting, ultrasonic cleaning, use of an abrasive water jet, and laser cleaning. Physical

methods are easy to deploy, but they are constrained by the thickness of the rust layer and the inevitable damage incurred on the bulk metals.

Conventionally, rust layers are removed by polishing or dissolving in acid solutions. However, the corrosion rate differs on different parts of the metal substrate, which results in a rough metal surface underneath the rust layer. Moreover, pitting corrosion can lead to a small hole in some local areas. In this case, rust cannot be uniformly removed by mechanical polishing or a deep hole will appear after dissolving the rust by chemical etching. Rather than removing the rust from the substrate, directly converting the rust to metal is another way to rehabilitate the corrosion layer. In general, rust mainly consists of oxides and hydroxides that can be reduced to metal by hydrogen, carbon, and reactive metals. However, hydrogen can dissolve in steel and cause hydrogen embrittlement, and carbothermic reduction requires a high temperature and sufficient contact between the rust and carbon. Moreover, carbon or reactive metals can change the composition of the metal substrate and thereby alter its physical properties. Electrochemical deoxidation employs electrons to reduce oxides to below a controlled potential, a technique that has been used to extract metals/alloys from oxides and

Corresponding author: Hua-yi Yin E-mail: yinhy@smm.neu.edu.cn

© University of Science and Technology Beijing 2021

sulfides [8–17]. In an electrochemical cell, solid oxides in the form of a porous pellet act as a cathode and are reduced to metals/alloys, releasing oxide ions into the electrolyte. The released oxide ions then transfer to the anode and are oxidized to oxygen at an inert anode [18–20]. Since the reduction of a solid oxide follows the principles of the three-phase interline model [21–23], surface reduction is quite fast and the rate-determining step is the diffusion of the oxide ions outward from the oxide core to the pre-metalized shell. Moreover, electrochemical reduction is not restricted by the shape of the cathode because the reduction occurs wherever the liquid electrolyte can reach. Therefore, this electrochemical process could provide an effective method for converting rust layers back to metals/alloys, i.e., repairing rather than removing the rust.

In other words, the electro-derusting method is a conversion method. Taking advantage of the rapid reduction rate of the thin oxide layer in molten salts [24–25], in this study, we used the electrochemical method to convert thin rust scale to metal, i.e., realizing electrochemical metalization of the rust. The use of electrons introduces no contaminants and the electrolyte is flowable, so the deoxidation process is not constrained by the shape of the object. For example, the rusty metal parts like a screw can be easily restored. Moreover, oxygen ions can be extracted from a tiny pitting hole because the diffusion of oxide ions is enabled by cathodic polarization. In this study, we achieved the electrochemical conversion of rust on the surface of iron/steels in molten $\text{Na}_2\text{CO}_3\text{--K}_2\text{CO}_3$ using a cost-effective Ni-based inert anode. We used cyclic voltammetry (CV) to investigate the electrochemical reduction behaviors of the rust.

2. Experimental

2.1. Cyclic voltammetry

For this experiment, the electrochemical cell was placed in an alumina crucible (inside diameter (ID): 9.4 cm, Height: 12.3 cm, Shanghai Shuocun Co., Ltd., China), which was housed in a one-end-closed stainless steel (SS) test vessel (ID: 12 cm, height: 60 cm). The test vessel was heated by a vertical tube furnace. Granular Na_2CO_3 and K_2CO_3 were mechanically mixed in a plastic bottle (Na_2CO_3 : K_2CO_3 = 59:41, molar ratio, analytical reagent grade, Kermel Co., Ltd., China). Then, the mixture was transferred into an Al_2O_3 crucible and vacuum-dried at 300°C for 12 h. Next, the Al_2O_3 crucible was placed into the SS test vessel while ramping up the temperature and flow of Ar gas to maintain an inert atmosphere for subsequent electrochemical measurements. After the salt was melted, pre-electrolysis was initiated between a nickel-sheet (2 cm × 2 cm) cathode and a Ni10Cu11Fe anode at a constant cell voltage of 1.8 V for 4 h. CV tests were performed using a three-electrode setup to investigate the electrochemical reduction behaviors of the iron rust. The

working electrode was a rusty-iron wire (ID: 0.5 mm), the counter electrode was a home-made Ni10Cu11Fe alloy (ID: 2 cm) [26–28], and the pseudo-reference electrode was an Ag wire (ID: 0.5 mm, >99.99%). The CV measurements were controlled by an electrochemical workstation (CHI 1140, Shanghai Chenhua, Co., Ltd., China).

2.2. Electrochemical derusting

The drying and pretreatment steps used on the molten salt were the same as those described above. The electrochemical derusting of the rust layer on the surface of an iron rod was performed in a two-electrode cell with the same molten $\text{Na}_2\text{CO}_3\text{--K}_2\text{CO}_3$ that was used in the CV measurement. The electrochemical derusting process was conducted in a two-electrode electrolytic cell with the molten $\text{Na}_2\text{CO}_3\text{--K}_2\text{CO}_3$ electrolyte (Fig. 1), with the rusty iron serving as the cathode and a Ni10Cu11Fe alloy as an inert anode [26,29–30]. Constant cell voltages were supplied between the cathode and anode via a battery testing system (Shenzhen Neware Co., Ltd., China, the maximum supply current and voltage for which are 6 A and 5 V, respectively). At a constant potential, the rust was electrochemically reduced to iron, releasing oxide ions into the electrolyte, whereupon the oxide ions diffused toward the anode where they were electrochemically oxidized to oxygen gas. As Ni10Cu11Fe has been confirmed to be a stable oxygen-evolution inert anode, the rust could be electrochemically converted to metal and oxygen, i.e., the rust was electrochemically converted to iron and oxygen in the molten salt.

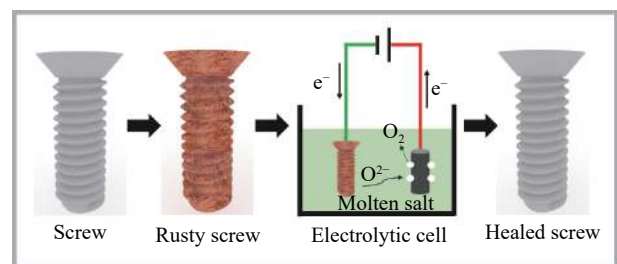


Fig. 1. Schematic of the electrochemical metalization of iron rust in molten $\text{Na}_2\text{CO}_3\text{--K}_2\text{CO}_3$.

2.3. Characterization

All the samples before and after electrolysis were characterized by scanning electron microscopy (SEM, FEI Quanta250FEG), energy dispersive X-ray spectroscopy (EDS), and X-ray diffraction (XRD, Shimadzu X-ray 6000 with Cu K_α radiation at $\lambda = 0.15405$ nm).

3. Results and discussion

To investigate the electrochemical reduction process, we used a fresh and a rusty-iron wire, respectively, as working

electrodes on which we performed CV measurements. Fig. 2(a) shows the deposition and stripping of Na from the fresh-iron-wire working electrode. On the rusty-iron-wire working electrode, two more reduction peaks appeared prior to the deposition of Na due to the reduction of the iron rust. The reduction behaviors are similar to the electrochemical-reduction behavior of iron oxide in molten $\text{Na}_2\text{CO}_3\text{-K}_2\text{CO}_3$ [31], which indicates that the rust on the iron mainly consisted of iron oxide. Note that the rust could contain some hydroxides or oxyhydroxide, which can be converted to oxide in high-temperature conditions. The reduction behaviors of iron oxide in molten $\text{Na}_2\text{CO}_3\text{-K}_2\text{CO}_3$ were studied [28,31]. As shown in Fig. 2(a), redox peaks c1'/a1' are attributable to the deposition and stripping of Na, and redox peaks c1/a1, c2/a2,

and c3/a3 are correlated with the reduction of Fe_2O_3 . Reduction peak c1 can be attributed to the formation of NaFe_2O_3 , and redox peaks c2/a2 correspond to the reduction process from NaFe_2O_3 to NaFeO_2 and Fe, and reduction peak c3 corresponds to the conversion of NaFeO_2 to Fe. On the reverse scan, the oxidation peaks could be due to the oxidation of Fe, NaFeO_2 , and NaFe_2O_3 . As shown in Fig. 2(b), the reduction peaks decreased significantly in the second scan because most of the iron rust had been reduced during the first scan. In the third scan, no oxidation peak occurred due to the lack of oxide ions in the vicinity of the working electrode, which means that the oxide ions released from the working electrode had diffused into the electrolyte and become oxidized at the counter electrode.

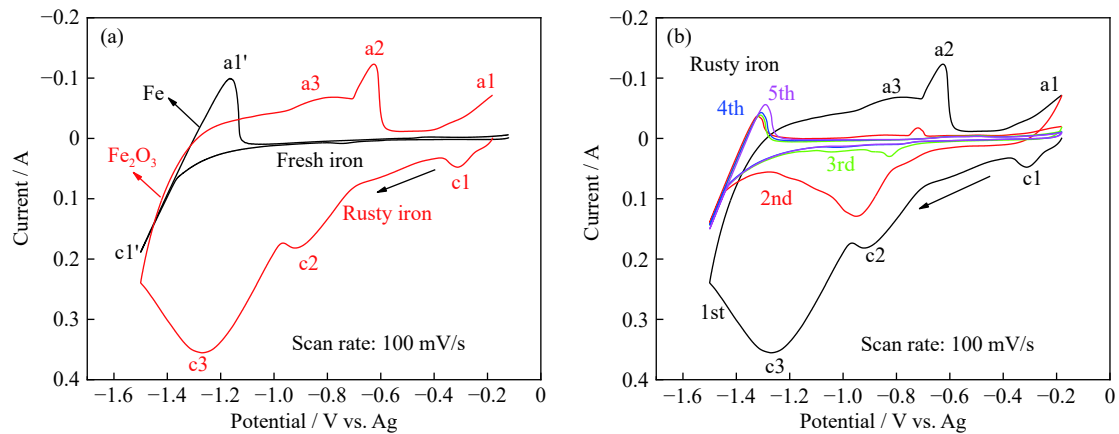


Fig. 2. Cyclic voltammograms of (a) fresh-iron-wire (black line) and rusty-iron-wire (red line) working electrodes, and (b) a rusty-iron-wire working electrode with multiple scans in molten $\text{Na}_2\text{CO}_3\text{-K}_2\text{CO}_3$ at 750°C and a scan rate of 100 mV/s .

As shown in Fig. 3(a), iron rust mainly comprises Fe_2O_3 . In addition to oxides, some undetected hydroxides or oxyhydroxide could exist in an amorphous state. In molten $\text{Na}_2\text{CO}_3\text{-K}_2\text{CO}_3$, NiO [32] and Co_3O_4 [30] have been successfully reduced to Ni and Co, meaning that the electrochemical derusting method could be applied to various metal

oxides. For reactive metals, the molten salts from a much wider electrochemical window could be applied, i.e., alkaline and alkaline-earth-based hydroxides [33–34], chlorides [35], and fluorides [36]. Moreover, by engineering the components of molten salts and controlling the applied potentials, the morphologies and carburization of the metal sub-

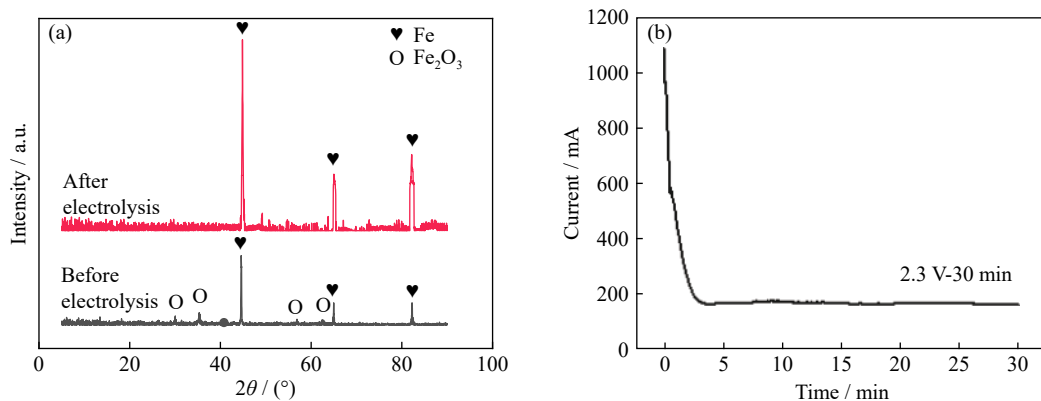


Fig. 3. (a) XRD patterns of a rusty iron rod before and after electrolysis, and (b) current profile of electrochemical derusting at a constant cell voltage of 2.3 V in molten $\text{Na}_2\text{CO}_3\text{-K}_2\text{CO}_3$ at 750°C .

strate could be tailored [20].

Prior to electrolysis, the iron rust on the samples was yellowish in color. After electrolysis, the yellowish samples become gray with a metallic luster (Fig. 4). The yellowish rod was observed to turn gray within 5 min, which indicates a fast reduction rate. As shown in Fig. 4, the Fe content exceeded 94at% after 5 min of electrolysis. The Na content was less than 1at% in all samples. We note that it is difficult to quantitatively measure the contents of C and O by EDS. From the current plot, we can see that the reduction current decreased to a plateau after 5 min (Fig. 3(b)).

As shown in Fig. 5, the iron rust layer was converted to interconnected iron particles, which confirms that the electrochemical reduction of iron rust was complete. Since the activity of iron increases with decreases in the size of the iron particle, the electrolytically metalized layer should be post-treated to form a perfect corrosion-resistant layer. In light of the improved chemical activity of the electro-metalized iron, this metalized layer could serve as a functional layer, such as a gas diffusion electrode [37–38]. In addition, iron rust has a

rough surface with bract-shape particles ranging from 1 to 5 μm in size (Fig. 5(a)). After electrolysis, these bract-shape particles are transformed into nodule-like particles, which are identical to the electrolytic Fe particles obtained from the electrolysis of solid Fe_2O_3 [28].

In general, the corrosion rate differs at different locations, which results in corrosion areas of different depths in different locations. Thus, the electrochemical approach is an effective way to restore a pitting point because the electrolyte can reach the pitted area and the applied electric field can drive the oxide ions from a deeply pitted hole. As shown in Figs. 5(b)–5(e), the rough surfaces of the electrolytic iron rod can be attributed to the different corrosion rates in different areas. From the cross-sectional SEM image (Fig. 6(a)), we can see that the thickness of the rust layer is $\sim 100 \mu\text{m}$. After electrolysis, the oxide layer becomes porous due to its deoxidation (Fig. 6(b)). The thickness of the resulting electrochemically metalized layer is almost the same as that of the original rust layer.

The electrochemically metalized material can facilitate

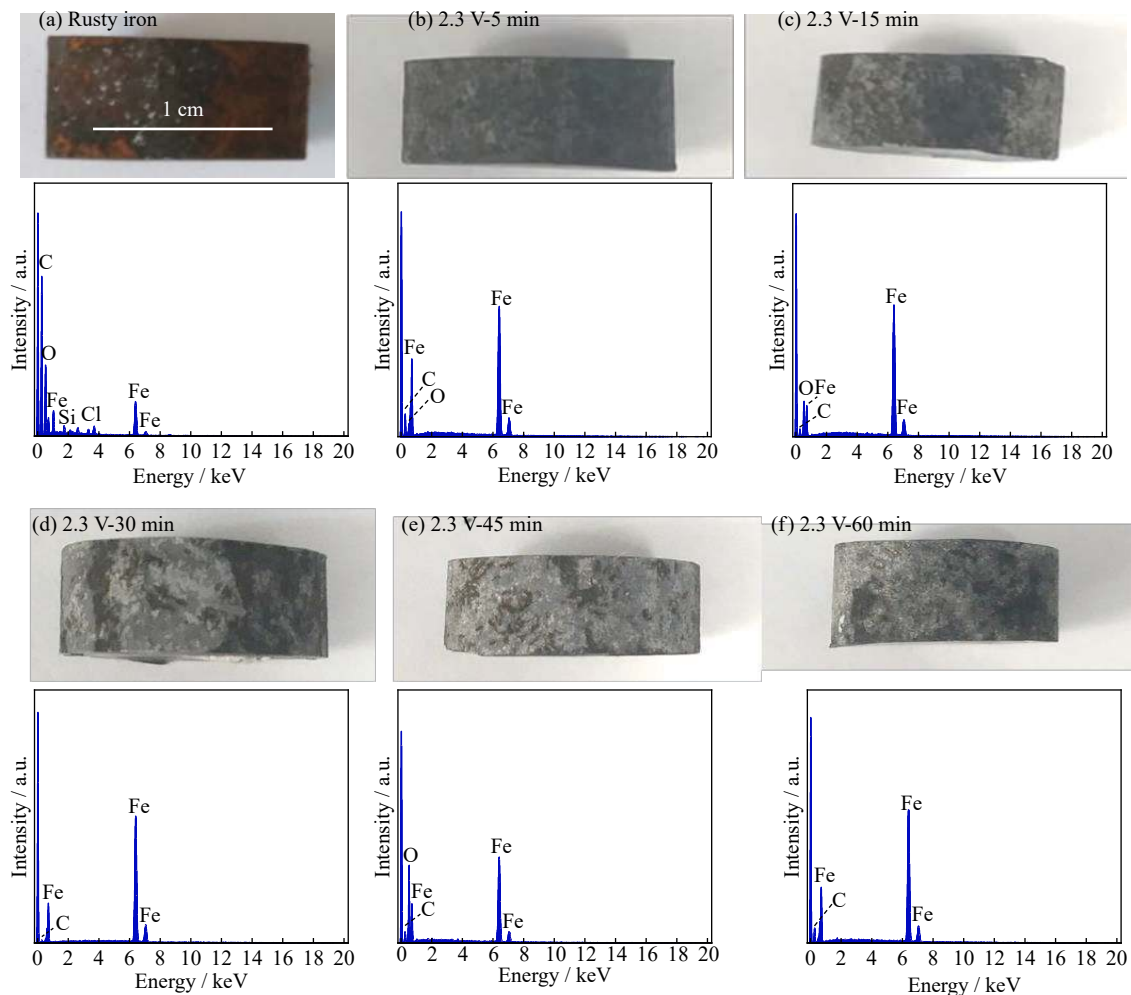


Fig. 4. Digital photographs and EDS analyses of (a) the rusty iron rods and samples after being electrolyzed at a constant cell voltage of 2.3 V for (b) 5 min, (c) 15 min, (d) 30 min, (e) 45 min, and (f) 60 min.

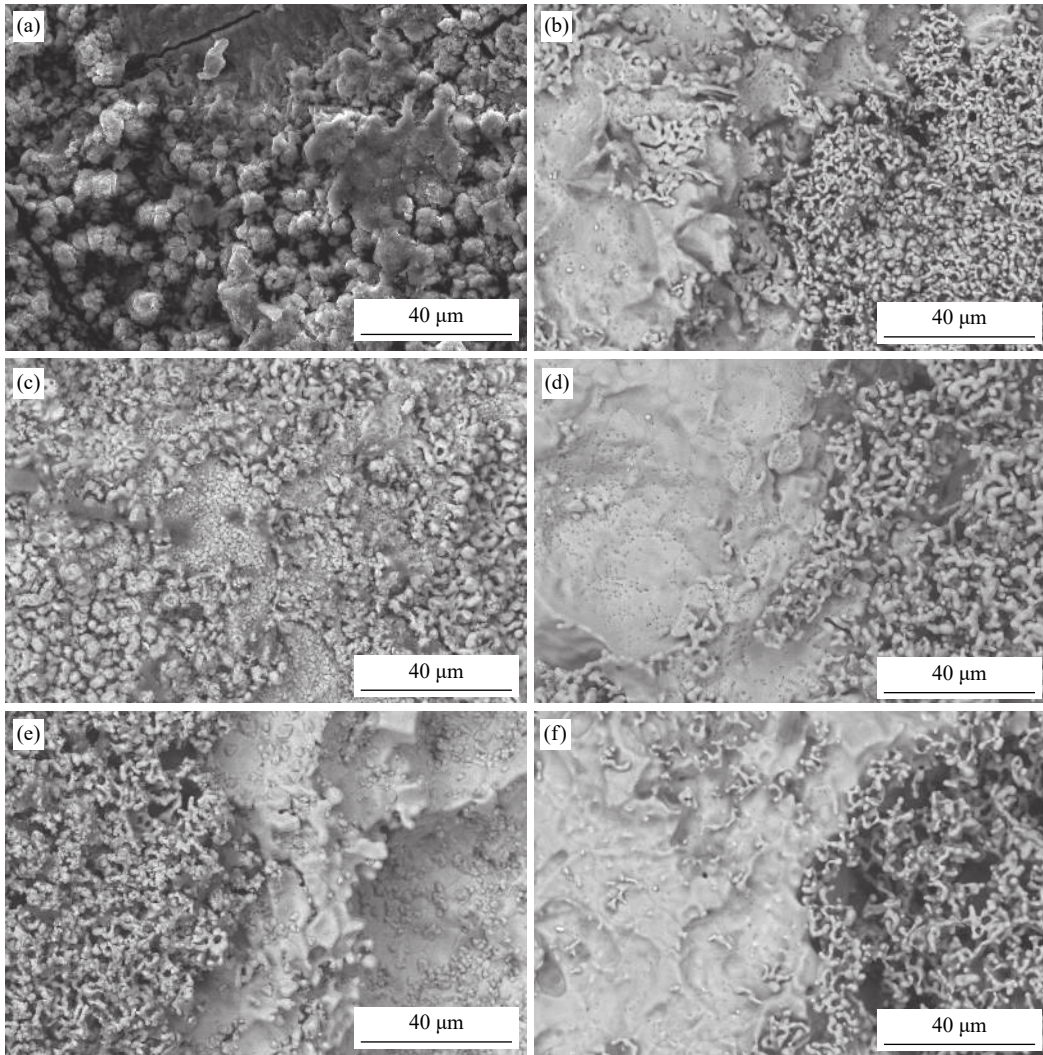


Fig. 5. SEM images of the rusty iron (a) and the rusty iron after being electrolyzed at a constant cell voltage of 2.3 V for (b) 5 min, (c) 15 min, (d) 30 min, (e) 45 min, and (f) 60 min.

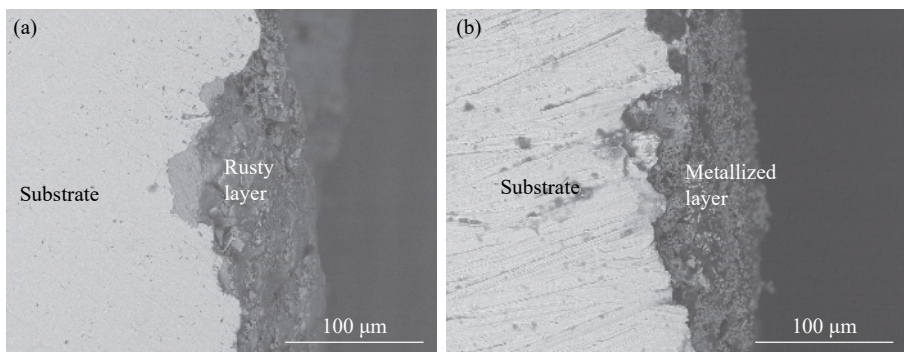


Fig. 6. Cross-sectional SEM images of (a) the rusty iron and (b) the rusty iron after being electrolyzed at a constant cell voltage of 2.3 V for 30 min.

machining, heat treatment, electroplating, and coating of an artificial corrosion-resistant layer. In addition, the reduction of the rust layer provides a potential way of producing three-dimensional porous structures for other applications. Moreover, the metalization reaction takes place at the inter-

face of the metal electrode/oxide/electrolyte. Thus, the electrochemical metalization technique could be applied in the machining of an insulative oxide layer by selective electrochemical reduction in molten salts.

In addition to the metalization of a rusty iron rod, we elec-

trochemically derusted a rusty screw in molten $\text{Na}_2\text{CO}_3\text{--K}_2\text{CO}_3$ (Fig. 7). The screw had a rough surface, with a thread depth (Fig. 7(a)) and slot depth (Fig. 7(b)) of ~ 1 mm and ~ 3 mm, respectively. After electrolysis, the rust on the screw was eliminated and, instead, a metallic luster appeared, which means the rust layer on the screw surface had been reduced back to metal (Figs. 7(c)–7(d)). Note that the rust in the slot had fully converted to metal, demonstrating that electrochemical metalization is not limited by the object shape. Hence, the electrochemical process can derust rusty objects of different shapes and structures wherever the electrolyte can reach. Although the electrochemical process is efficient, the surface of the repaired iron is porous and can be reoxidized. For objects with irregular shape and roughness, the distribution of current at the electrode should be considered. The electrochemical derusting approach can be combined with certain surface technologies to prevent further corrosion.

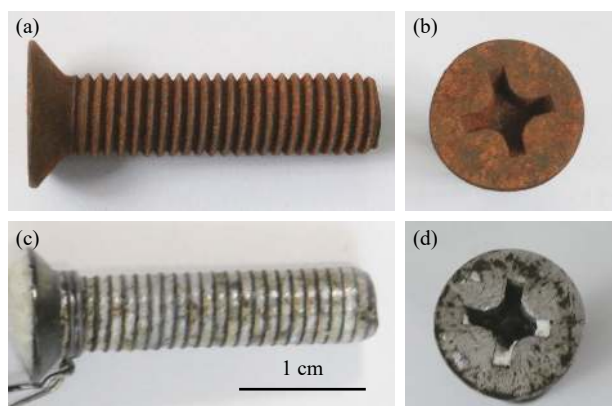


Fig. 7. Digital photographs of the rusty screws before (a, b) and after electrolysis (c, d) at a constant cell voltage of 2.3 V for 30 min in molten $\text{Na}_2\text{CO}_3\text{--K}_2\text{CO}_3$ at 750°C .

4. Conclusion

This paper reported the demonstration of an electrochemical derusting route in molten $\text{Na}_2\text{CO}_3\text{--K}_2\text{CO}_3$. Iron rust primarily consisting of iron oxide can be electrochemically reduced to iron via a two-step process. At a constant cell voltage of 2.3 V, rust was electrochemically metalized in 5 min. This derusting process is applicable to rusty objects of various shapes and structures. Moreover, the electrochemical derusting reaction can be tailored by adjusting the applied cell voltage and electrolyte. Note that the electrochemically metalized iron is porous so a post-treatment is necessary to prevent re-corrosion. This method could represent an alternative way to repair specific metal objects and to recover their original appearance rather than removing the rust layer. Overall, the electrochemical metalization approach offers a promising way to repair various rusty metals/alloys and cultural relics.

Acknowledgements

This work is financially supported by the Fundamental Research Funds for the Central Universities (No. N172505002), the National Natural Science Foundation of China (No. 51704060), the National Thousand Youth Talent Program of China, and the 111 Project (No. B16009).

References

- [1] J. de Beer, E. Worrell, and K. Blok, Future technologies for energy-efficient iron and steel making, *Annu. Rev. Energy Env.*, 23(1998), No. 1, p. 123.
- [2] S.J. Oh, D.C. Cook, and H.E. Townsend, Characterization of iron oxides commonly formed as corrosion products on steel, *Hyperfine Interact.*, 112(1998), No. 1-4, p. 59.
- [3] H. Tamura, The role of rusts in corrosion and corrosion protection of iron and steel, *Corros. Sci.*, 50(2008), No. 7, p. 1872.
- [4] Z.M. Wang, X.Y. Zeng, and W.L. Huang, Parameters and surface performance of laser removal of rust layer on A3 steel, *Surf. Coat. Technol.*, 166(2003), No. 1, p. 10.
- [5] Z.L. Tang, A review of corrosion inhibitors for rust preventative fluids, *Curr. Opin. Solid State Mater. Sci.*, 23(2019), No. 4, art. No. 100759.
- [6] V. Narayanan, R.K. Singh, and D. Marla, Laser cleaning for rust removal on mild steel: An experimental study on surface characteristics, [in] *The 3rd International Conference on Design and Manufacturing Engineering*, Vol. 221, 2018, Melbourne, p. 01007.
- [7] A. Azhari, C. Schindler, K. Hilbert, C. Godard, and E. Kersch, Influence of waterjet peening and smoothing on the material surface and properties of stainless steel 304, *Surf. Coat. Technol.*, 258(2014), p. 1176.
- [8] G.Z. Chen, D.J. Fray, and T.W. Farthing, Direct electrochemical reduction of titanium dioxide to titanium in molten calcium chloride, *Nature*, 407(2000), No. 6802, p. 361.
- [9] A.M. Abdelkader, K.T. Kilby, A. Cox, and D.J. Fray, Voltammetry of electro-deoxidation of solid oxides, *Chem. Rev.*, 113(2013), No. 5, p. 2863.
- [10] S.L. Wang and Y.J. Li, Reaction mechanism of direct electro-reduction of titanium dioxide in molten calcium chloride, *J. Electroanal. Chem.*, 571(2004), No. 1, p. 37.
- [11] A. Allanore, L. Yin, and D.R. Sadoway, A new anode material for oxygen evolution in molten oxide electrolysis, *Nature*, 497(2013), No. 7449, p. 353.
- [12] T. Wang, H.P. Gao, X.B. Jin, H.L. Chen, J.J. Peng, and G.Z. Chen, Electrolysis of solid metal sulfide to metal and sulfur in molten NaCl--KCl , *Electrochem. Commun.*, 13(2011), No. 12, p. 1492.
- [13] H.Y. Yin, B. Chung, and D.R. Sadoway, Electrolysis of a molten semiconductor, *Nat. Commun.*, 7(2016), art. No. 12584.
- [14] J.K. Qu, H.W. Xie, Q.S. Song, Z.Q. Ning, H.J. Zhao, and H.Y. Yin, Electrochemical desulfurization of solid copper sulfides in strongly alkaline solutions, *Electrochem. Commun.*, 92(2018), p. 14.
- [15] S.Q. Jiao and H.M. Zhu, Novel metallurgical process for titanium production, *J. Mater. Res.*, 21(2006), No. 9, p. 2172.
- [16] R.O. Suzuki, M. Aizawa, and K. Ono, Calcium-deoxidation of niobium and titanium in Ca-saturated CaCl_2 molten salt, *J. Alloys Compd.*, 288(1999), No. 1-2, p. 173.

- [17] D. Hu, A. Dolganov, M.C. Ma, B. Bhattacharya, M.T. Bishop, and G.Z. Chen, Development of the Fray-Farthing-Chen Cambridge process: towards the sustainable production of titanium and its alloys, *JOM*, 70(2018), No. 2, p. 129.
- [18] H.W. Xie, H.J. Zhao, Q.S. Song, Z.Q. Ning, J.K. Qu, and H.Y. Yin, Anodic gases generated on a carbon electrode in oxide-ion containing molten CaCl₂ for the electro-deoxidation process, *J. Electrochem. Soc.*, 165(2018), No. 14, p. E759.
- [19] D.H. Wang, A.J. Gmitter, and D.R. Sadoway, Production of oxygen gas and liquid metal by electrochemical decomposition of molten iron oxide, *J. Electrochem. Soc.*, 158(2011), No. 6, p. E51.
- [20] N.J. Siambun, H. Mohamed, D. Hu, D. Jewell, Y.K. Beng, and G.Z. Chen, Utilisation of carbon dioxide for electro-carburisation of mild steel in molten carbonate salts, *J. Electrochem. Soc.*, 158(2011), No. 11, p. H1117.
- [21] W. Xiao, X.B. Jin, Y. Deng, D.H. Wang, and G.Z. Chen, Three-phase interlines electrochemically driven into insulator compounds: A penetration model and its verification by electroreduction of solid AgCl, *Chem. Eur. J.*, 13(2007), No. 2, p. 604.
- [22] W. Xiao, X.B. Jin, Y. Deng, D.H. Wang, and G.Z. Chen, Rationalisation and optimisation of solid state electro-reduction of SiO₂ to Si in molten CaCl₂ in accordance with dynamic three-phase interlines based voltammetry, *J. Electroanal. Chem.*, 639(2010), No. 1-2, p. 130.
- [23] W. Xiao, X.B. Jin, Y. Deng, D.H. Wang, X.H. Hu, and G.Z. Chen, Electrochemically driven three-phase interlines into insulator compounds: Electroreduction of solid SiO₂ in molten CaCl₂, *Chem. Phys. Chem.*, 7(2006), No. 8, p. 1750.
- [24] E. Gordo, G.Z. Chen, and D.J. Fray, Toward optimisation of electrolytic reduction of solid chromium oxide to chromium powder in molten chloride salts, *Electrochim. Acta*, 49(2004), No. 13, p. 2195.
- [25] W. Xiao and D.H. Wang, The electrochemical reduction processes of solid compounds in high temperature molten salts, *Chem. Soc. Rev.*, 43(2014), No. 10, p. 3215.
- [26] X.H. Cheng, L. Fan, H.Y. Yin, H. Liu, K.F. Du, and D.H. Wang, High-temperature oxidation behavior of Ni–11Fe–10Cu alloy: Growth of a protective oxide scale, *Corros. Sci.*, 112(2016), p. 54.
- [27] X.H. Cheng, H.Y. Yin, and D.H. Wang, Rearrangement of oxide scale on Ni–11Fe–10Cu alloy under anodic polarization in molten Na₂CO₃–K₂CO₃, *Corros. Sci.*, 141(2018), p. 168.
- [28] H.Y. Yin, D.Y. Tang, D. Zhu, Y. Zhang, and D.H. Wang, Production of iron and oxygen in molten K₂CO₃–Na₂CO₃ by electrochemically splitting Fe₂O₃ using a cost affordable inert anode, *Electrochem. Commun.*, 13(2011), No. 12, p. 1521.
- [29] D.Y. Tang, K.Y. Zheng, H.Y. Yin, X.H. Mao, D.R. Sadoway, and D.H. Wang, Electrochemical growth of a corrosion-resistant multi-layer scale to enable an oxygen-evolution inert anode in molten carbonate, *Electrochim. Acta*, 279(2018), p. 250.
- [30] X.H. Cheng, D.D. Tang, H. Zhu, and D.H. Wang, Cobalt powder production by electro-reduction of Co₃O₄ granules in molten carbonates using an inert anode, *J. Electrochem. Soc.*, 162(2015), No. 6, p. E68.
- [31] D.Y. Tang, H.Y. Yin, W. Xiao, H. Zhu, X.H. Mao, and D.H. Wang, Reduction mechanism and carbon content investigation for electrolytic production of iron from solid Fe₂O₃ in molten K₂CO₃–Na₂CO₃ using an inert anode, *J. Electroanal. Chem.*, 689(2013), p. 109.
- [32] D.Y. Tang, H.Y. Yin, X.H. Cheng, W. Xiao, and D.H. Wang, Green production of nickel powder by electroreduction of NiO in molten Na₂CO₃–K₂CO₃, *Int. J. Hydrogen Energy*, 41(2016), No. 41, p. 18699.
- [33] A. Allanore, H. Lavelaine, G. Valentin, J.P. Birat, and F.M. Lapique, Iron metal production by bulk electrolysis of iron ore particles in aqueous media, *J. Electrochem. Soc.*, 155(2008), No. 9, p. E125.
- [34] A. Cox and D.J. Fray, Electrolytic formation of iron from haematite in molten sodium hydroxide, *Ironmaking Steelmaking*, 35(2008), No. 8, p. 561.
- [35] D.H. Wang, X.B. Jin, and G.Z. Chen, Solid state reactions: An electrochemical approach in molten salts, *Annu. Rep. Prog. Chem. Sect. C*, 104(2008), p. 189.
- [36] F. Lantelme and H. Groult, *Molten Salts Chemistry: From Lab to Applications*, vol. 28, Elsevier, Amsterdam, 2013.
- [37] N. Linares, A.M. Silvestre-Albero, E. Serrano, J. Silvestre-Albero, and J. García-Martínez, Mesoporous materials for clean energy technologies, *Chem. Soc. Rev.*, 43(2014), No. 22, p. 7681.
- [38] M.Y. Wang, X.T. Yu, Z. Wang, X.Z. Gong, Z.C. Guo, and L. Dai, Hierarchically 3D porous films electrochemically constructed on gas–liquid–solid three-phase interface for energy application, *J. Mater. Chem. A*, 5(2017), No. 20, p. 9488.